Active battery cell equalization using a Flyback converter with current mode control

Manuel Rico-Secades, Pablo Quintana-Barcia, Emilio L. Corominas, Antonio J. Calleja, and Javier Ribas

ce^3i^2 research group, University of Oviedo, Spain

Email: mrico@uniovi.es

Abstract

Due to different charge and discharge rates, temperature gradients and coulomb efficiencies, cells in series-connected battery/ultracapacitor packs may have diverse voltage levels. Therefore, equalization stages are essential to extend its lifetime and reduce significant impacts like overcharged cells. This work presents an active equalization stage based on a Flyback converter with current mode control valid for both series-connected battery and ultracapacitor banks. Unlike most of the methods that can be found in the bibliography, expensive bidirectional power switches are not necessary and recirculation of energy is avoided. With just a mesh of bipolar transistors and optocouplers it is possible to equalize all the cells of the battery/ultracapacitor bank, presenting a low-cost active solution. In addition, a design methodology of the proposed system detailing prominent specifications is included in this work along with simulation and experimental results.

Index Terms

Energy storage, cell equalization, Lithium batteries, ultracapacitors, Flyback converter, current mode control

I. Introduction

MEETING the Mandatory Renewable Energy Target (MRET) of 20% by 2020 could be significantly easier if battery energy storage systems (BESS) were integrated and deeply entrenched in renewable energy sources (RES). In fact, BESS combined with PV systems will be fundamental for the continued incorporation of domestic PV installations [1]. It is well known that PV systems connected directly to a low voltage supplier can occasionally cause overvoltage issues [2]. In some countries there are specific regulations to disconnect automatically whether maximum voltage levels are surpassed [3], [4]. Different methods are available today to solve these situations, e.g. reduction of active power injection into the grid and instead, energy storage.

Therefore, batteries and ultracapacitors are key elements. Battery cells and ultracapacitors nominal voltage is usually small (3.2 V for Li-Fe cells, 3.7 for Li-ion or 2.7 for ultracapacitors). Hence, they are required to be assembled in large series modules in order to store or recover significant amounts of energy, which indeed is quite a challenge [5]. Fig. 1 shows a set of batteries and ultracapacitors, including the well-known standard 18650 for Li-ion batteries.

Indeed, these kind of devices outperform the more traditional NiMH and lead-acid batteries, in terms of higher energy and power densities, higher charge/discharge efficiency, and longer lifetime [6]. Given these outstanding advantages, Li-ion batteries portray a valid solution for energy storage applications where the battery consists of several cells connected to achieve the required energy and power levels [6], [7].

Fig. 1: Set of batteries and ultracapacitors

However, maximum and minimum cell voltages must be strictly controlled for both, batteries and ultracapacitors technologies. The charging process of a pack of BESS must stop immediately if one cell reaches the maximum voltage value. Similarly, during the BESS pack discharge, if a cell comes to the minimum voltage value, the process has to finish. Therefore, a perfect equalization of the cells of a BESS pack allows to fully charge or completely recover the stored energy in a battery/ultracapacitor bank.

Numerous cell equalization methods have been proposed during these past years. Some of them can be found in the bibliography. Generally speaking, they make use of expensive and difficult to control bidirectional switches, multiwinding transformers or switched capacitor techniques [8]–[12].

The aim of this paper is to propose a simpler, low-cost active equalization method, as depicted shaded in gray in Fig. 2. It consists of an 8 series connected batteries/ultracapacitors bank (from C_1 to C_8), a so-called battery module cell selector and low power current contolled Flyback converter. The proposal is easy to integrate in conventional BESS along with the main bidirectional converter and the protection circuitry (PCM in Fig. 2).

This paper is organized as follows: In Section II, the main features of the proposed active cell equalizer are presented. Then, Section III explores the cells voltage measurement and the transistors switching strategy while the analysis and optimal design of the converter that equalize the BESS is detailed in Section IV. In Section V, an in-depth explanation of different control
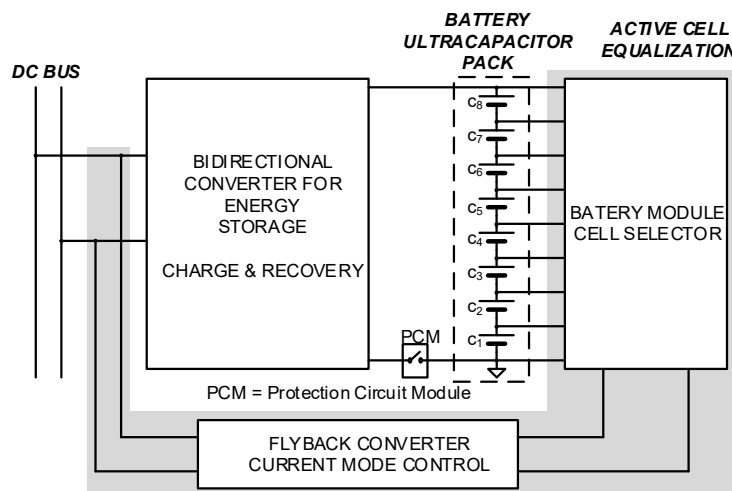

Fig. 2: Active Cell equalization proposal

strategies for BESS equalization using the proposed system is done along with several simulation results. Finally, Section VI shows some experimental results that validate the proposal while conclusions and future developements are reached in Section VII.

II. Features of the proposed active cell equalizer

All power modules of Fig. 2 have been replaced by equivalent current sources in Fig. 3. I_{bat} substitutes the interface module between the BESS and the DC bus that operates either as a battery charger or as an energy recovery system from the batteries. On the other hand, I_{eq} performs the equalization stage of the battery/ultracapacitor bank. The cell with lower voltage would be connected directly to this current source through a mesh of bipolar transistors and diodes (battery module cell selector). For the purpose of cells equalization, a proper input and output switches configuration has to be chosen. For instance, if cell C_5 is the one with the lowest voltage, then input switches I_{e_7}, I_{e_6} and I_{e_5} as well as output switches I_{s_5}, I_{s_4}, I_{s_3} and I_{s_2} need to be turned on. This way, the equalization current (I_{eq}) flows only across cell C_5. Obviously, a constant monitoring of the voltage of the cells is required.

This equalization method has several advantages over classic methods, e.g. switched capacitors ([13], [14]). Some of the most outstanding are the following:

- Fast switching and bidirectional switches are not required on the battery module cell selector. It is possible to stop the equalization current ($I_{eq} = 0$) anytime and change the transistors configuration so as to charge a different cell.

- Energy recirculation is not required in this method. The energy can be obtained from the external DC bus and therefore, it is not necessary to extract it from one cell to inject it again in a different one. The efficiency of the equalization process can hence be increased.

- A fast equalization can be implemented with low power requirements. Cells maximum voltages are usually low and the equalization current (I_{eq}) can be as high as required to speed the process up. In addition, it is possible to program different current equalization levels according to the unbalancing voltage in the cells.
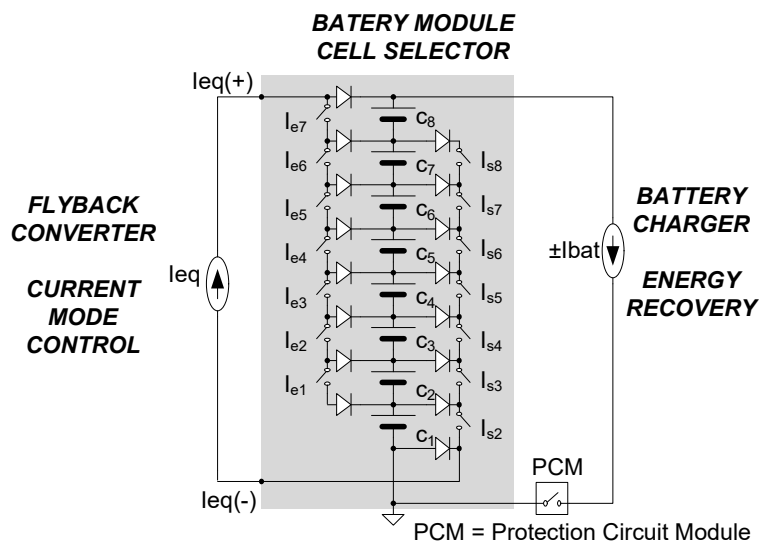

Fig. 3: Basic schematic of the active cell equalization proposal

III. Cells voltage measurement and cell selection for equalization

The first step to implement the strategy presented in Fig. 3 is to measure the voltage of each cell (V_{CELL_j}). Fortunately, voltage changes are slow in these devices and current microcontroller units (MCU) can easily read several analog inputs. Then, a low cost solution for low voltage cell measurement has been implemented using resistances of identical value, as seen in Fig. 4. The only condition they have to fulfill is that they all must have the same value.

All leg voltage measurements (V_{L_j}) are referred to the negative terminal of the battery bank and they have to be performed sequentially: firstly, leg 1 (V_{L_1}) to obtain directly the voltage of cell 1. Then, V_{L_2} has to be quantified in order to calculate the voltage of cell 2 and so on until the last cell, applying (1).

$$V_{L_i} = \frac{\sum_{j=1}^{i} V_{CELL_j}}{i} \tag{1}$$

For instance, the calculation of the voltage of C_2 in Fig. 4 can be done as follows (2):

$$V_{CELL_2} = 2V_{L_2} - V_{CELL_1} \tag{2}$$

As for the battery module cell selector, it is implemented through a mesh of bipolar transistors (PNP) and optocouplers, as shown in Fig. 5. In this way, the control of the PNP transistors is using optocouplers referred to the negative terminal of the BESS. They are well-suited for this application since they are easy to control and can drive enough current to equalize the batteries. The equalization process is thus, the following:

1) Stop the equalization current ($I_{eq} = 0$).
2) Switch on the proper transistors with the MCU in order to select the battery.
3) Turn on again the converter and begin the equalization operation.

IV. Optimal design of the power converter for the equalization stage

To implement the equalization current source I_{eq}, a floating voltage in both output terminals of the power converter is required. Then, a Flyback converter is an excellent solution for this application considering the low-power levels required [15].
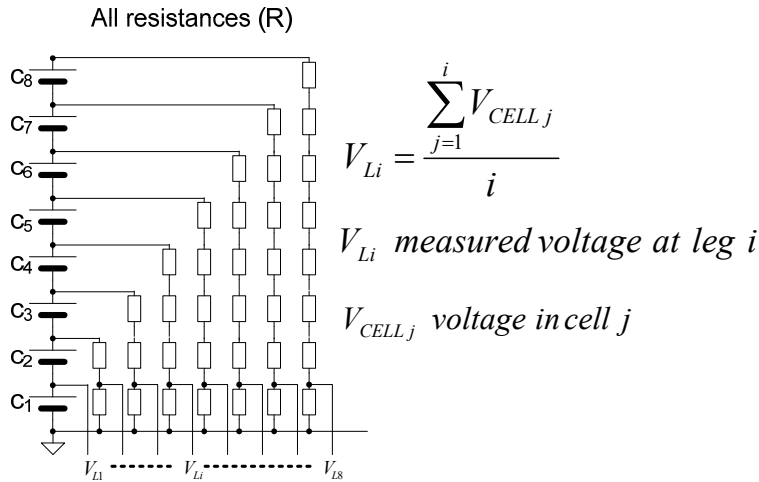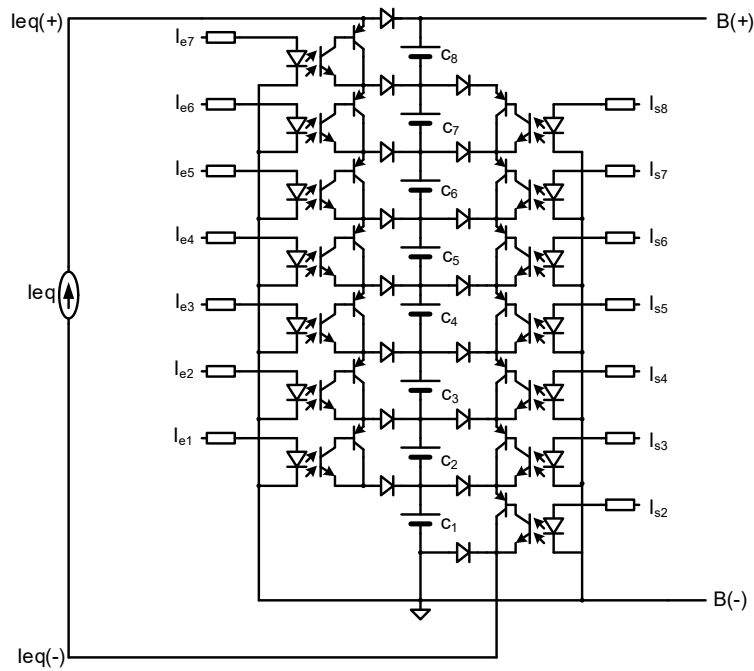

Fig. 4: Voltage cell measurement strategy

Fig. 5: Battery module cell selector using bipolar transistors and optocouplers

The control framework of this converter needs to be a current control strategy in order to fixed a certain output current. The authors decided to use a fixed off-time technique. The basic idea is to obtain a constant off-time when the power MOSFET is turned off and a variable on-time. It should be noted that this design approach is quite simple and cost-effective, because the constant off-time is easily set by an RC circuit. The MOSFET is turned on until the current across reaches the maximum specified value ($I_{T_{MAX}}$) as depicted in Fig. 6.

To properly design this small power unit and its control strategy. However, it is mandatory to previously define the DC bus voltage (V_{BUS}) which will provide the energy to the equalization converter and the voltage limits of each cell (V_{CELL}):
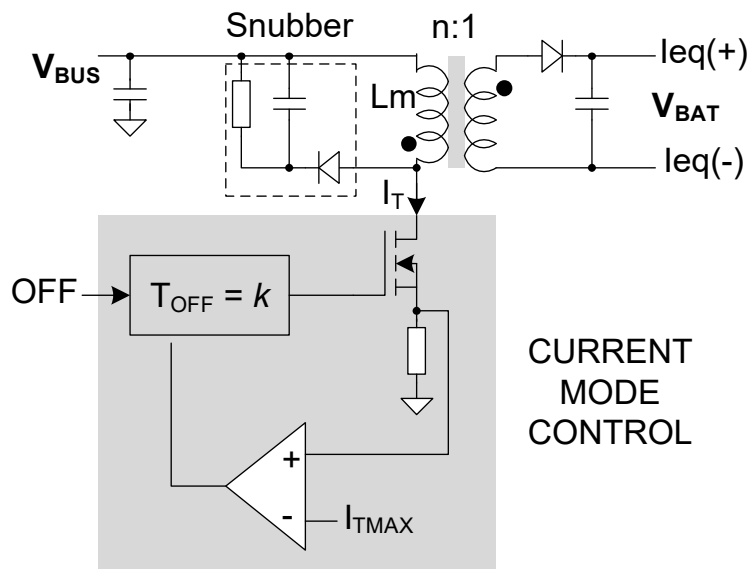

Fig. 6: Current mode control Flyback for BESS equalization

Step 1: *Select the turns ratio of the Flyback (n:1)*

The common choice of the Flyback turns ratio value is that one that fulfills that the duty cycle remains close to 0.5 operating in nominal conditions ($V_{CELL_{NOM}}$ and $V_{BUS_{NOM}}$). The relationship between these parameters is shown in (3):

$$d = \frac{n \cdot V_{CELL}}{V_{BUS} + n \cdot V_{CELL}} \tag{3}$$

where d is the duty ratio and n the turns ratio.

However, there are many considerations that must be taken into account before choosing the suitable turns ratio, i.e. fluctuations in the DC bus and/or the cells voltages as well as the voltage drop in the transistors and diodes when they are forward biased. In Fig. 7 an example of how these fluctuations affect the whole analysis is presented where $V_{BUS} = 48 \pm 5$V. A turns ratio $n = 13$ yields to a duty ratio close to 0.5, similar to the target value.

Step 2: T_{OFF} *selection*

As mentioned before herein, the control strategy is based on a fixed off-time technique. It implies the switching frequency (F_s) to not be constant and it varies depending on different parameters. The relation between F_s and T_{OFF} is shown in (4) in continuous conduction mode (CCM):

$$F_s = \frac{1 - d}{T_{OFF}} \tag{4}$$

where T_{OFF} is the fixed off-time.

Considering the previous turns ratio calculation and a T_{OFF} value of 10 μs, the evolution of F_s can be calculated upon different cell and DC bus voltages (Fig. 8). As depicted, an operation region within 40 and 60 kHz is obtained. Moreover, it should be noted that the lower T_{OFF}, the higher F_s.

Step 3: *Choosing the magnetizing inductance (L_m) of the Flyback transformer*

The magnetizing inductance current ripple (ΔI) depends on the own inductance value, L_m, as expressed in (5):

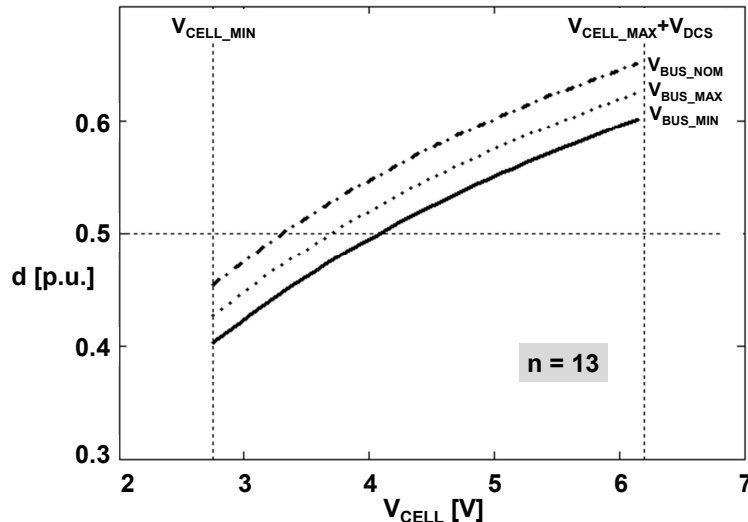$$L_m = \frac{n \cdot V_{BAT} \cdot T_{OFF}}{\Delta I} \tag{5}$$

Fig. 7: Duty cycle fluctuations for $n = 13$. Li-ion battery cell ($V_{MAX} = 4.2$V, $V_{NOM} = 3.7$V and $V_{MIN} = 2.75$V) and DC bus voltage 48 ± 5V

Higher L_m values mean lower current ripples and considering T_{OFF} is a constant value, ΔI depends basically on the battery voltage, V_{BAT}. Again, the voltage drop in the semiconductors (transistors, diodes, etc.) need to be considered. In this work, taking into account manufacturers' datasheets, a value of $V_{DCS} = 2$V (voltage drop cell selector) was chosen to increment the range of the output voltage under study. This parameter is the addition of the voltage drop in the switched on bipolar PNP transistors and the forward biased diodes. The evolution of the current ripple in a magnetizing inductor of $1mH$ considering all previously obtained parameters is shown in Fig. 9.

Step 4: *Maximum current through power MOSFET ($i_{T_{MAX}}$)*

The equalization average output current ($I_{OUT_{AVG}}$) can be regulated by controlling the power switch peak current ($I_{T_{MAX}}$). This relationship can be expressed as:

$$I_{OUT_{AVG}} = n \cdot \frac{2 \cdot I_{T_{MAX}} - \Delta I}{2} \cdot (1 - d) \tag{6}$$

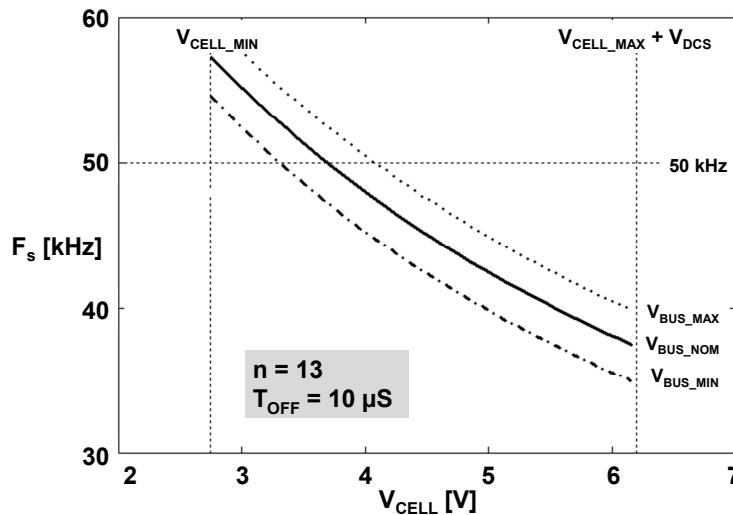Equation (6) can be also expressed graphically for a $I_{T_{MAX}} = 0.4$A as depicted in Fig. 10a.

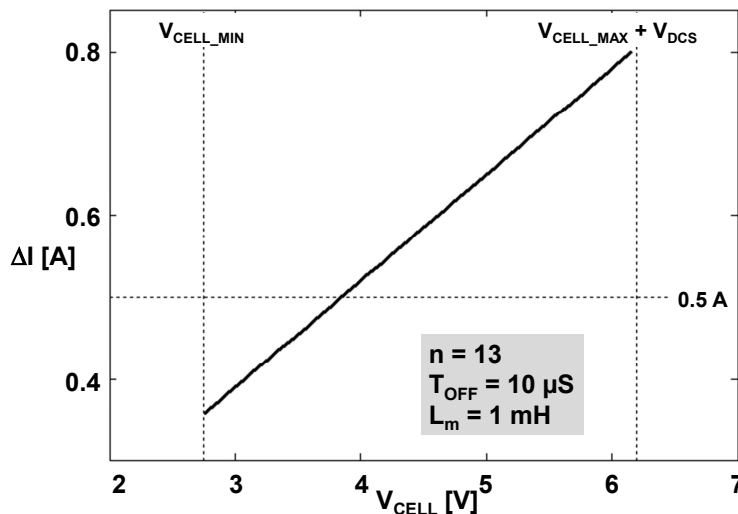Fig. 8: Switching frequency (F_s) values for different cell and DC bus voltages

Fig. 9: Evolution of the magnetizing inductance current ripple for $L_m = 1mH$

Several important conclusions can be obtained from these figures. Firstly, Flyback current mode control presents a behavior similar to a current source in open loop. Second, average output current decreases slightly if cell voltage increases, which it is favorable from the equalization point of view.

There is a third interesting issue: as shown in Fig. 10b, the relation between the average output current and the peak current of the power transistor is linear. Hence, it allows for the possibility that this $I_{T_{MAX}}$ parameter can be used in closed-loop operation and also to modify the equalization current depending on the cells voltage.

Finally, one of the particular characteristics of fixed off-time control is that it works no matter if the converter is in CCM or DCM. Therefore, for a fixed maximum current of 0.4 A through the transistor, the power converter would work in both operating modes depending on the voltage of the cell due to the allowed current ripple of Fig. 9.

V. CONTROL STRATEGIES AND SIMULATION RESULTS

Taking into account today's MCU capabilities, four different strategies have been proposed in the present work. These strategies modify how the equalization is done and they have been denoted as EQUA-CATCH, EQUA-TIME, CHAR-CATCH and CHAR-TIME. In the following paragraphs, these operation modes are in-depth explained along with simulations in PSIM. For simplicity, the battery storage elements were assumed to be capacitors with high capacity storage [16]. Moreover, the extra
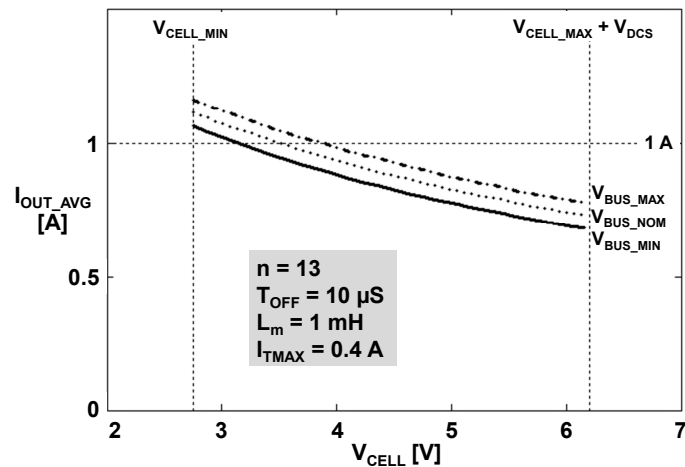
(a)
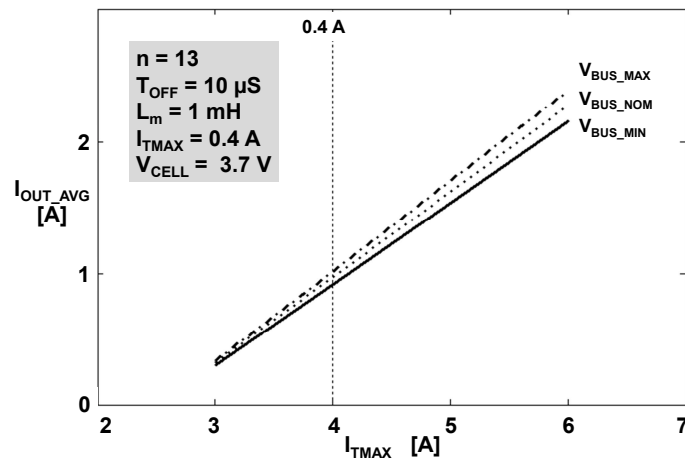
(b)

Fig. 10: (a) Average output current evolution for $I_{T_{MAX}} = 0.4$A. (b) Relationship between average output current and peak current at power switch

output variable, *status*, indicates which cell is currently absorbing energy, if there is one. For instance, if $status = 0$, no cell is charging or being equalized. On the other hand, if $status = 1$ it means cell 1 is draining the current. It has also been programmed a time delay of 100 ms between the charging process of two cells in order to change the transistors configuration and turn on again the converter. Finally, owing to reduce time simulation, only four batteries in series were simulated.

The four different equalization/charging strategies are therefore explained ahead:

EQUA-CATCH **operation mode:** The system is configured to equalize all the cells. The one with the lowest voltage is selected by the MCU and then, the equalization current is directly applied to it. This process continues until this cell's voltage reaches the highest one in the battery stack. This operation is done repeatedly until the difference between maximum and minimum voltage among all the cells is below a certain tolerance value. Fig. 11a shows an example of this operation mode. At the beginning, the MCU detects the cell with the lowest value, switches on the correspondent PNP transistors and then turns on the converter. It can be noted that the one with lowest voltage is cell 3 ($status = 3$). Therefore, the control charges this cell until it reaches the maximum voltage cell value. In this case, it corresponds to cell 4. Later, the converter stops and the MCU changes the transistors configuration in order to charge the next cell and so on until all of them have a similar value within a certain tolerance.

EQUA-TIME **operation mode:** In this operation mode, instead of looking for the lowest cell voltage and rise it to the highest one, the system finds the lowest and injects current in that cell during a certain time. Fig. 11b presents this operation mode. At the starting point, cell 3 is again the one with the lowest voltage. It charges during a certain time until next cell, in this case, cell 2 becomes the one with the lowest value and begins to drain the equalization current. Unlike EQUA-CATCH mode, cells are charged in a more coordinated way.

CHAR-CATCH **operation mode:** In this case, the system operates in cell-by-cell charger mode. Hence, it no longer works as an equalizer but as a charger. This means that this operation mode looks for the cell with lowest voltage and charge it until the maximum value allowed. In the example of Fig. 11c, cells are charged sequentially to the maximum allowed for Li-ion batteries: 4.2V. This operation mode is not recommendable when the BESS is being discharged at the same time.

CHAR-TIME **operation mode:** This operation mode charges the cells to the maximum tolerated but during an established time. The process is repeated continuously until all the cells are fully charged. Unlike the previous mode, this one is suitable to support the BESS whether it is being discharged. Fig. 11d illustrates this mode.

VI. EXPERIMENTAL VALIDATION

The proposed methodology has also been implemented in the battery modules of the electric vehicle (EV) of UNIOVI team at Formula Student competition [17].

But first, experiments have been carried out to verify the feasibility of the proposed approach. A laboratory prototype has been built using Li-ion batteries series connected, as presented in Fig. 12a. This prototype consists of two cell packs for future developments. In the present work, only one pack was used. Two different boards were built in order to run the experiment. One of them includes the power converter and the battery module selector. The control board is plugged in upon the first one, as shown in Fig. 12b.

Moreover, Table I summarizes the main parameters of the built prototype, including information about the power converter and battery module cell selector components.

In order to characterize the Flyback converter, a first laboratory experiment was performed using a resistive load of 2Ω. The transistor voltage and inductor current waveforms are shown in Fig. 13a. The converter operates in CCM, providing 1A to

TABLE I: Prototype parameters

Battery module	
Standard of cell	18650
Nominal capacity	12000 mAh
Nominal voltage	3.7 V
Maximum voltage	4.2 V
Minimum voltage	2.75 V
Cells in series per pack	8
Total energy stored at 100% DOD (Depth of discharge)	355 Wh
Total energy stored at 80% DOD	284 Wh
Converter and battery module selector	
DC link nominal voltage	48 ± 5V
Switching frequency	35-60 kHz
Equalization current (avg)	1A
PNP transistors	FMMT717
Optocoupler	TLP-181
Flyback power mosfet	TK5P60W
Flyback magnetizing inductor	$1m$H
Shottky diodes (battery module cell selector)	B260A-13-F
Microcontroller unit	dsPIC30F6015

the load. In addition, a second experiment was carried out. This time, the load was one of the proposed batteries. As seen in Fig. 13b, due to the cell voltage, the converter changes its operation point and starts working in DCM. Even though changes in the load may appear, the fixed off-time control allows the converter to work and be regulated either in CCM or DCM without affecting the average output current value.

VII. Conclusions and future developments

In this paper, a current equalization method for serially connected battery cells has been presented. With this method, recirculation of energy is avoided and bidirectional power switches are not required. A fixed off-time Flyback converter was chosen to perform the equalization process. This converter operates both in DCM and CCM tracking the current reference indifferently. In addition, several control strategies were presented in this work, allowing to choose between using the converter as an equalization stage or as a charger. Compared to other methods, the proposed scheme requires low-cost elements and it stands out by its simplicity and high reliability. In future works, the failure detection in cells can be included as well as different control strategies. In addition, wireless cell monitoring is currently under study [18].

## Acknowledgment

References

[1] T. M. Jackson, G. R. Walker, and N. Mithulananthan, "Integrating pv systems into distribution networks with battery energy storage systems," in *2014 Australasian Universities Power Engineering Conference (AUPEC)*, Sept 2014, pp. 1–7.

[2] J. Tant, F. Geth, D. Six, P. Tant, and J. Driesen, "Multiobjective battery storage to improve pv integration in residential distribution grids," *IEEE Transactions on Sustainable Energy*, vol. 4, no. 1, pp. 182–191, Jan 2013.

[3] M. Braun, T. Stetz, R. Brndlinger, C. Mayr, K. Ogimoto, H. Hatta, H. Kobayashi, B. Kroposki, B. Mather, M. Coddington, K. Lynn, G. Graditi, A. Woyte, and I. MacGill, "Is the distribution grid ready to accept large-scale photovoltaic deployment? state of the art, progress, and future prospects," *Progress in Photovoltaics: Research and Applications*, vol. 20, no. 6, pp. 681–697, 2012. [Online]. Available: http://dx.doi.org/10.1002/pip.1204

[4] *Automatic disconnection device between a generator and the public low-voltage grid*, DIN VDE 0126-1-1 Std., August 2013.

[5] R. B. Bass, J. Carr, J. Aguilar, and K. Whitener, "Determining the power and energy capacities of a battery energy storage system to accommodate high photovoltaic penetration on a distribution feeder," *IEEE Power and Energy Technology Systems Journal*, vol. 3, no. 3, pp. 119–127, Sept 2016.

[6] F. Baronti, C. Bernardeschi, L. Cassano, A. Domenici, R. Roncella, and R. Saletti, "Design and safety verification of a distributed charge equalizer for modular li-ion batteries," *IEEE Transactions on Industrial Informatics*, vol. 10, no. 2, pp. 1003–1011, May 2014.

[7] W. Su, H. Eichi, W. Zeng, and M. Y. Chow, "A survey on the electrification of transportation in a smart grid environment," *IEEE Transactions on Industrial Informatics*, vol. 8, no. 1, pp. 1–10, Feb 2012.

[8] H. S. Park, C. H. Kim, K. B. Park, G. W. Moon, and J. H. Lee, "Design of a charge equalizer based on battery modularization," *IEEE Transactions on Vehicular Technology*, vol. 58, no. 7, pp. 3216–3223, Sept 2009.

[9] H. S. Park, C. E. Kim, C. H. Kim, G. W. Moon, and J. H. Lee, "A modularized charge equalizer for an hev lithium-ion battery string," *IEEE Transactions on Industrial Electronics*, vol. 56, no. 5, pp. 1464–1476, May 2009.

[10] Y. Shang, C. Zhang, N. Cui, and J. M. Guerrero, "A cell-to-cell battery equalizer with zero-current switching and zero-voltage gap based on quasi-resonant lc converter and boost converter," *IEEE Transactions on Power Electronics*, vol. 30, no. 7, pp. 3731–3747, July 2015.

[11] P. A. Cassani and S. S. Williamson, "Design, testing, and validation of a simplified control scheme for a novel plug-in hybrid electric vehicle battery cell equalizer," *IEEE Transactions on Industrial Electronics*, vol. 57, no. 12, pp. 3956–3962, Dec 2010.

[12] C. H. Kim, M. Y. Kim, H. S. Park, and G. W. Moon, "A modularized two-stage charge equalizer with cell selection switches for series-connected lithium-ion battery string in an hev," *IEEE Transactions on Power Electronics*, vol. 27, no. 8, pp. 3764–3774, Aug 2012.

[13] C. Pascual and P. T. Krein, "Switched capacitor system for automatic series battery equalization," in *Proceedings of APEC 97 - Applied Power Electronics Conference*, vol. 2, Feb 1997, pp. 848–854 vol.2.

[14] Y. Yuanmao, K. W. E. Cheng, and Y. P. B. Yeung, "Zero-current switching switched-capacitor zero-voltage-gap automatic equalization system for series battery string," *IEEE Transactions on Power Electronics*, vol. 27, no. 7, pp. 3234–3242, July 2012.

[15] R. W. Erickson, *Fundamentals of Power Electronics*, 2nd ed. Springer, January 2001.

[16] Y.-S. Lee and M.-W. Cheng, "Intelligent control battery equalization for series connected lithium-ion battery strings," *IEEE Transactions on Industrial Electronics*, vol. 52, no. 5, pp. 1297–1307, Oct 2005.

[17] J. A. del Valle, "Active equalization system based on flyback converter for the battery modules of the electric vehicle prototype of formula student uniovi team," *Workrooms Journal*, vol. 5, July 2017.

[18] N. Huerta-Medina, E. L. Corominas, P. J. Quintana, and M. R. Secades, "Smart control for smart grids: From lighting systems to grid side management," in *2016 13th International Conference on Power Electronics (CIEP)*, June 2016, pp. 104–109.
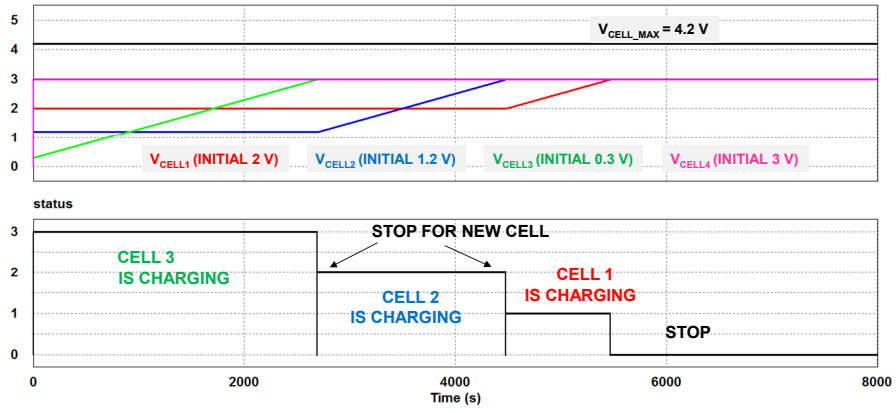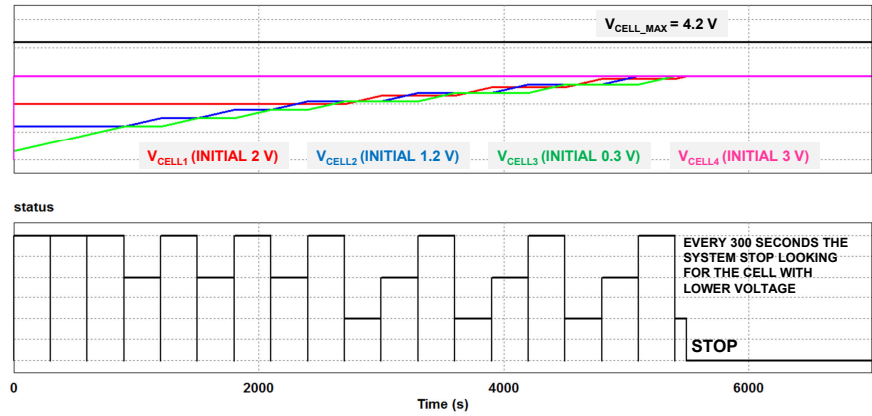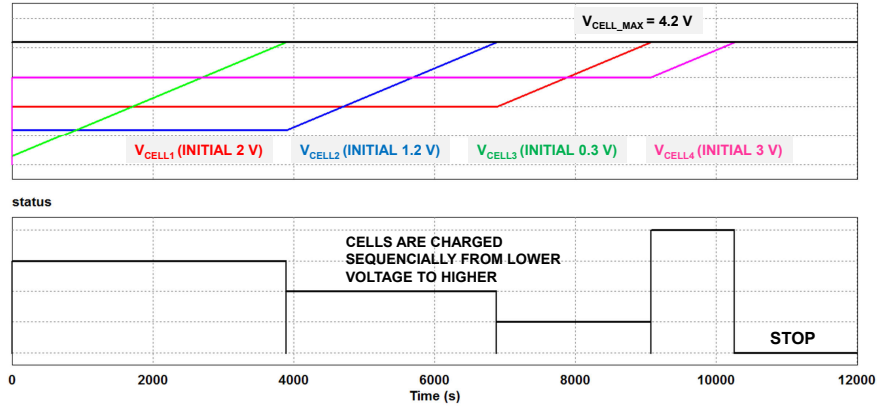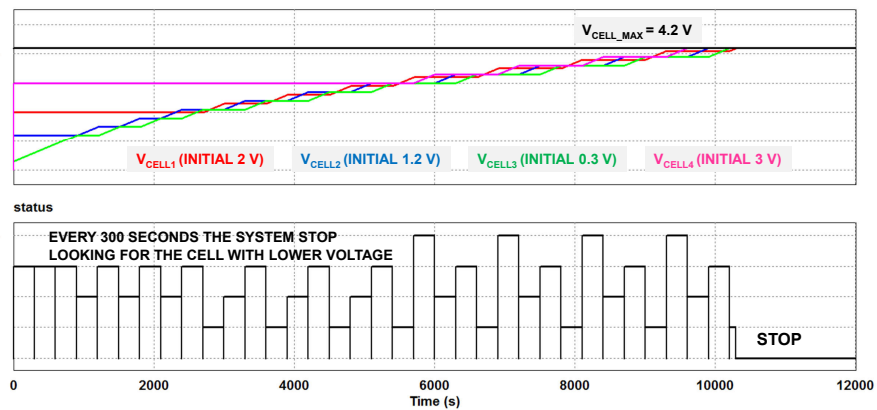
Fig. 11: (a) EQUA-CATCH (b) EQUA-TIME (c) CHAR-CATCH and (d) CHAR-TIME operation modes
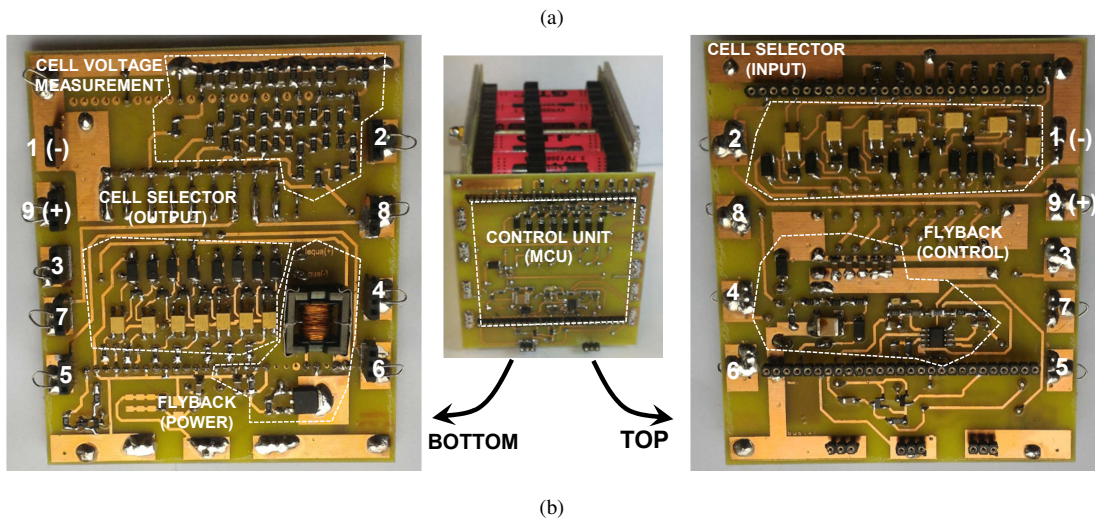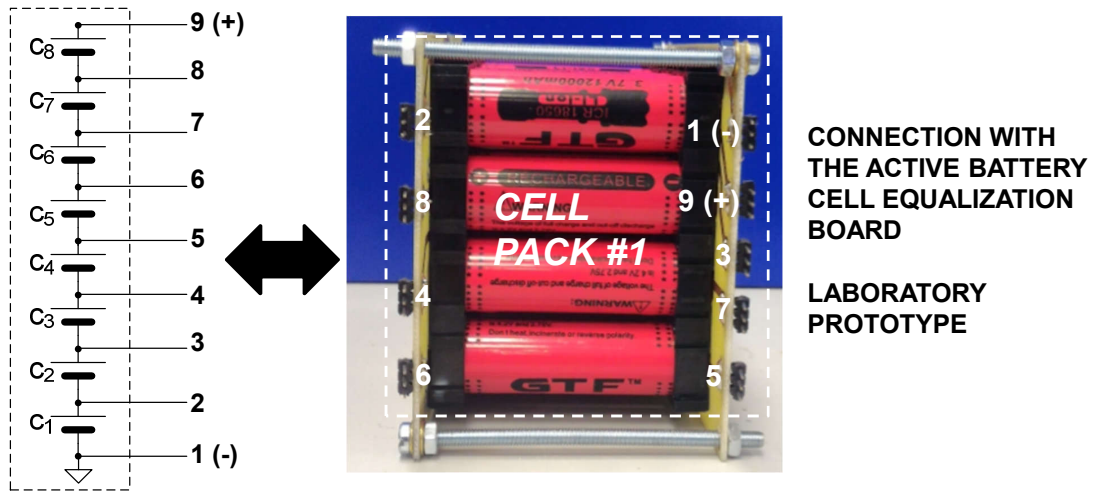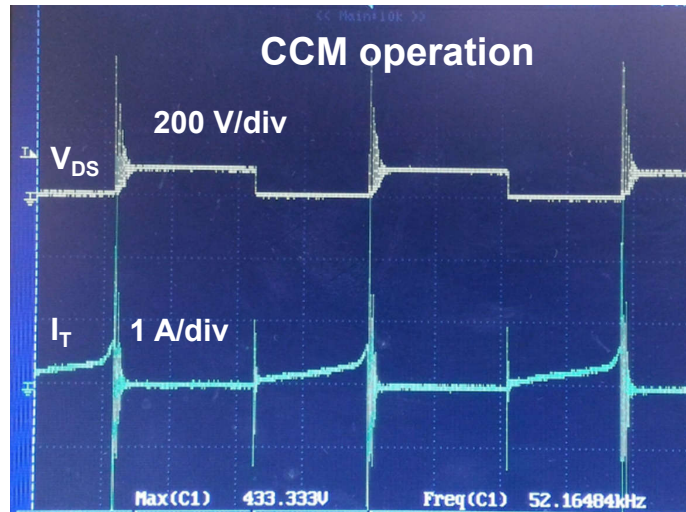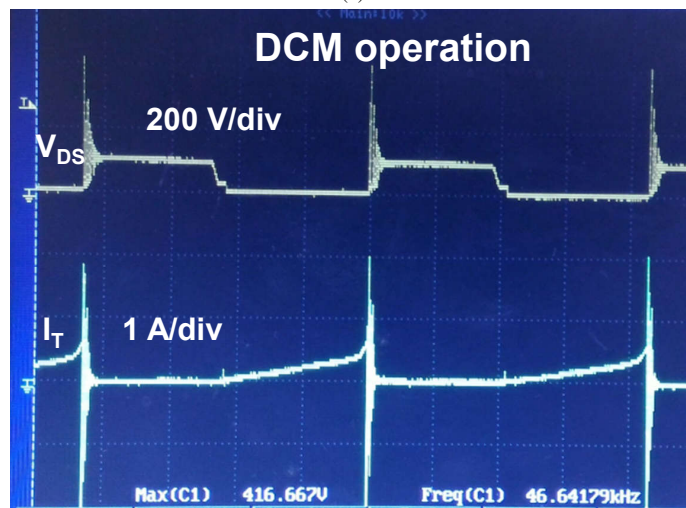
(a)

(b)

Fig. 12: (a) Energy storage module with two battery packs. Each pack consist of eight Li-ion cells. (b) Power converter, battery module selector and MCU PCBs

(a)

(b)

Fig. 13: Experimental results of the converter injecting power upon two different loads. CH1: (yellow; 200V/div) voltage drain-source of the power mosfet. CH2: (green, 1A/div) inductor current. Time/div: 5μs (a) Load: 2Ω resistance. (b) Load: Li-ion battery cell